Biophysical Chemistry 143 (2009) 85–94

Contents lists available at ScienceDirect

Biophysical Chemistry

journal homepage: http://www.elsevier.com/locate/biophyschem

A kinetic model for the metabolism of the herbicide safener fenclorim in *Arabidopsis thaliana*

Junli Liu *, Melissa Brazier-Hicks, Robert Edwards

School of Biological and Biomedical Sciences, Durham University, South Road, Durham DH1 3LE, UK

ARTICLE INFO

Article history:
Received 2 March 2009
Received in revised form 9 April 2009
Accepted 10 April 2009
Available online 24 April 2009

Keywords:
Glutathione conjugation
Glutathione transferases (GSTs)
Regulation
Dynamics
Oscillation
Xenobiotic detoxification

ABSTRACT

Glutathione transferases (GSTs) catalyse the detoxification of a range of xenobiotics, including crop protection agents in plants. Recent studies in cultures of the model plant *Arabidopsis thaliana* have shown that the herbicide safener fenclorim (4,6-dichloro-2-phenylpyrimidine) is conjugated by GSTs acting in the cytosol which are induced in response to this chemical treatment. The primary glutathione conjugates are then hydrolyzed to *S*-(4-chloro-2-phenylpyrimidin-6-yl)-cysteine, which after accumulating transiently in the cells and medium is then metabolized by a series of competing lyases and transferases, including GSTs, to a series of polar derivatives. This system therefore represents an example of an inducible metabolic pathway, where GSTs are involved in multiple steps and where detailed information on the content of intermediates is available. Using this data, a kinetic model describing the biotransformations of differing concentrations of fenclorim in *Arabidopsis* has been established, which was able to quantitatively analyse fluxes and changes in metabolite levels over time as a function of the induction of GSTs by the safener. The model confirmed a regulatory role for GSTs and the hydrolytic enzymes acting on the resulting glutathione conjugates. In addition, model analysis indicated that fenclorim metabolism is capable of generating oscillations if kinetic parameters are allowed to vary. The model offers new insights into the metabolic regulation of inducible xenobiotic metabolism in plants which is important in both determining herbicide selectivity in cereal crops and the remediation of organic pollutants by plants.

1. Introduction

Many herbicides used to control grass weeds in cereals are formulated and co-applied with safeners,which enhance xenobiotic metabolism and detoxification in the crop, thereby enhancing selectivity [1]. Safeners act by transcriptionally activating the expression of genes encoding several classes of detoxifying enzymes, notably the glutathione transferases (GSTs). Thus, the safening of several classes of graminicides including the chloroacetanilides and thiocarbamates, as well as important examples of sulfonyl urea and aryloxyphenoxypropionate herbicides used in cereal crops can be ascribed to the chemical induction of GSTs [2,3].

With an interest in determining the mechanism of safener action, we have recently studied the uptake and disposition of fenclorim (4,6-dichloro-2-phenylpyrimidine; Fig. 1) in cell and root cultures of the model plant *Arabidopsis thaliana* [4]. Fenclorim was originally developed to safen chloroacetanilide herbicides in rice, where it induces the expression of GSTs [5]. More recently, fenclorim has also been shown to be an effective inducer of GSTs in root and suspension cultures of *Arabidopsis* [6,7], with the safener undergoing glutathionylation catalyzed by GSTs [4]. In *Arabidopsis*, the glutathione conjugates of fenclorim undergo a series of proteolytic and conjugating reactions, including a secondary round of GST-mediated glutathionylation, to form a series of polar metabolites (Fig. 1). As such, fenclorim both activates the expression of GSTs as well as being acted on by these enzymes at several stages in the course of its metabolism. The metabolism of fenclorim in *Arabidopsis* therefore represents an intriguing paradigm to study the potential for self-regulation of inducible GST-mediated xenobiotic metabolism in plants. Such studies are of potential interest in both crop protection and phytoremediation, as several xenobiotics, including pollutants and herbicides, are known to self-enhance their metabolism in plants [6].

With an interest in developing a model to describe self-inducing detoxification pathways in plants we have taken data derived from *Arabidopsis* suspension cultured cells fed with fenclorim where we know the detoxifying GSTs are induced. We have then used the data derived from measuring the metabolites of the safener at timed intervals to address several questions. Specifically, why do the metabolites accumulate differentially over time? How does the trend relate to the kinetics of enzymes involved? To what extent is change in metabolic flux due to an increase in GST activity? Also, what dynamic properties does fenclorim metabolism exhibit? The objective of this work is therefore to

* Corresponding author. Tel.: +44 191 334 1376; fax: +44 191 334 1201.
E-mail address: junli.liu@durham.ac.uk (J. Liu).

0301-4622/$ – see front matter © 2009 Elsevier B.V. All rights reserved.
doi:10.1016/j.bpc.2009.04.006

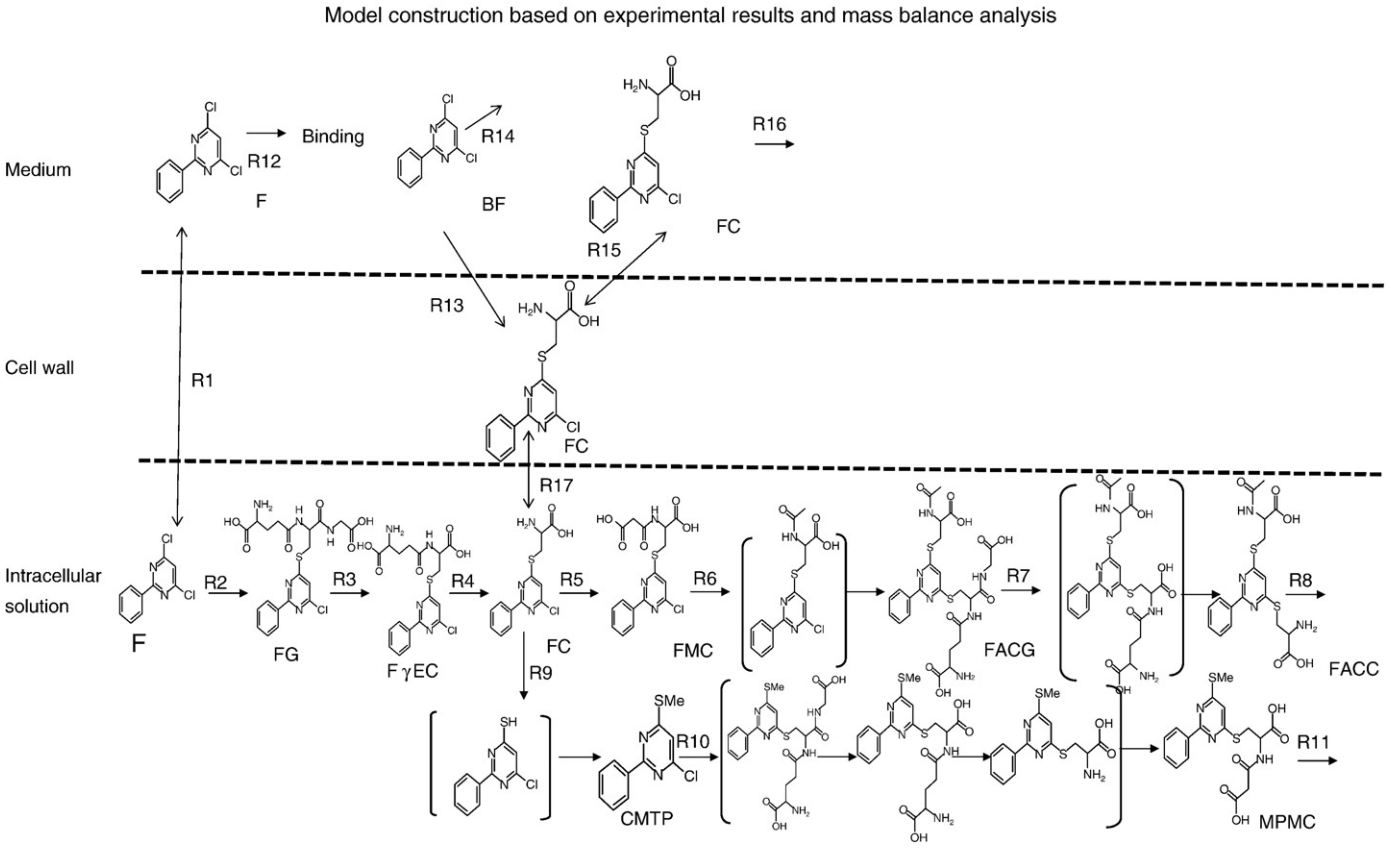

Fig. 1. Model for the metabolism of fenclorim in *Arabidopsis* cultures. Based on experimental evidence [4] and mass balance analysis, the model includes three compartments: the medium, the cell wall, and the intracellular solution. The abbreviations used are: GST, glutathione S-transferase; G, glutathione; CMTP, 4-chloro-6-(methylthio)-2-phenylpyrimidine; F, fenclorim (4,6-dichloro-2-phenylpyrimidine); FAC, S-(4-chloro-2-phenylpyrimidin-6-yl)-N-acetylcysteine; FACC, S-(4-N-acetylcysteine-2-phenylpyrimidin-6-yl)-cysteine;FACG, S-(4-N-acetylcysteine-2-phenylpyrimidin-6-yl)-glutathione; FC,S-(4-chloro-2-phenylpyrimidin-6-yl)-cysteine; FG, S-(4-chloro-2-phenylpyrimidin-6-yl)-glutathione; FγEC, S-(4-chloro-2-phenyl-pyrimidin-6-yl)-γ-glutamylcysteine; FMC, S-(4-chloro-2-phenylpyrimidin-6-yl)-N-malonylcysteine; MPMC, S-(4-(methylthio)-2-phenylpyrimidin-6-yl)-N–malonylcysteine. BF: unmeasured molecule (s) that is required based on mass balance.

integrate the biological knowledge of fenclorim metabolism into a kinetic model which can quantitatively address these questions.

2. A kinetic model for metabolism of herbicide safener fenclorim

2.1. Model development

As recently reported [4], the metabolism of fenclorim in *Arabidopsis* is well described with the reactions in the intracellular solution as shown (Fig. 1). The biotransformation of the safener is initiated by its GST-mediated conjugation to form *S*-fenclorim-glutathione (FG; *S*-(4-chloro-2-phenylpyrimidin-6-yl)-glutathione). The resulting conjugate is then sequentially acted on by a carboxypeptidase to produce (FγEC; *S*-(4-chloro-2-phenyl-pyrimidin-6-yl)-γ-glutamylcysteine) and then undergoes loss of the g-glutamyl group to yield the fenclorim-cysteinyl conjugate (FC; *S*-(4-chloro-2-phenylpyrimidin-6-yl)-cysteine). The carboxypeptidase activity is due to the action of the enzyme phytochelatin synthase [8,9]. Initially it was conjectured that the loss of the glutamate was catalysed through transpeptidation [4], though recent studies now suggest that the enzyme g-glutamyl cyclotransferase is more important in degrading glutathione and related conjugates in *Arabidopsis* [10]. FC is then subject to several competing processing reactions, notably i) *N*-malonylation to form FMC (*S*-(4-chloro-2-phenylpyrimidin-6-yl)-*N*-malonylcysteine); ii) the concerted action of a C-S lyase and *S*-methyltansferase to produce CMTP (4-chloro-6-(methylthio)-2-phenylpyrimidine); or iii) a secondary cycle of *S*-glutathionylation and proteolyic processing resulting in FACG (*S*-(4-N-acetylcysteine-2-phenylpyrimidin-6-yl)-glutathione), FACC (*S*-(4-N-acetylcysteine-2-phenylpyrimidin-6-yl)-cysteine), and MPMC (*S*-(4-(methylthio)-2-phenylpyrimidin-6-yl)-N-malonylcysteine). At a primary level, a kinetic model which describes the metabolism of fenclorim *in planta* needs to take into account a number of known biochemical factors which regulate this glutathione conjugation pathway. Firstly, the concentrations of GSTs will increase with time after fenclorim is applied, due to enhanced transcription/ translation of the respective genes [4]. These GSTs will catalyse both the primary conjugation of the safener as well as be involved in the secondary processing of the cysteine conjugates. Secondly, GSTs are subject to potent feed-back inhibition through the resulting glutathione conjugates acting as potent competitive inhibitors [11]. Originally, it was conjectured that once formed in plants, the glutathione conjugates were removed from the cytosol where the GSTs are located and deposited into the vacuole by ATP-binding cassette transporter proteins [12]. This would then impose a potential regulatory role for the transported in controlling GST-mediated conjugation. However, recent studies in *Arabidopsis* have now challenged this view and instead it is believed that the hydrolytic processing of the glutathione conjugates occurs predominantly in the cytosol [8–10]. In this revised model, the proteolytic processing of these glutathione conjugates to the respective peptide derivatives in the same compartment where they are formed would therefore be important in ensuring that feedback inhibition by the immediate reaction products of the GSTs does not occur.

Based on this biochemical knowledge and the measurement of fenclorim metabolites a model could be derived (Fig. 1). The associated reactions, enzymes involved and kinetics are described in Tables 1 and 2 respectively. The model construction process is as follows.

Table 1
Reactions in the model.

Reaction	Reaction description	Enzyme	Kinetics
R1: F in medium <—> F in cell	Fenclorim transport between medium and intracellular solution	Unknown	Reversible Michaelis Menten. Fenclorim transport process is reversible [4].
R2: F + G —> FG	Substitution with glutathione	Glutathione transferase (GSTs)	Conjugation kinetics of fenclorim and glutathione with F, FMC, and CMTP competing for available GSTs [4,13].
R3: FG—>FγEC + Glycine	Removal of glycine moiety	Phytochelatin synthase (PCS)	Irreversible Michaelis Menten, [4] and this work.
R4: FγEC —> FC+ γ-glutamyl	Removal of γ-glutamyl moiety	γ-Glutamyl-cyclotransferase	Irreversible Michaelis Menten, [4] and this work.
R5: FC + Malonyl-CoA —> FMC	Conjugation with malonyl moiety	*N*-malonyltransferase (NMT)	Irreversible Michaelis Menten, [4] and this work.
*R6: FMC +G —> FACG +carboxyl	Lumping two reactions: decarboxylation of FMC to FAC and conjugation of glutathione to FAC	Unknown enzyme for decarboxylation; Glutathione transferase (GSTs) for addition of glutathione	Conjugation kinetics of FMC and glutathione with F, FMC, and CMTP competing for available GSTs [4,13].
*R7: FACG —> FACC + Glycine + γ-glutamyl	Lumping two reactions: removal of glycine moiety and removal of γ-glutamyl moiety	Phytochelatin synthase and γ-Glutamyl-cyclotransferase	Irreversible Michaelis Menten, [4] and this work.
R8: FACC —>	Removal of FACC	Unknown	Mass action, this work.
*R9: FC + methyl —>CMTP + cysteinyl	Lumping two reactions: removal of cysteinyl moiety and addition of methyl moiety	C-S lyase and *S*-methyltransferase	Irreversible Michaelis Menten, [4] and this work.
*R10: CMTP +G —> MPMC + glycine + γ-glutamyl	Lumping three reactions: conjugation with glutathione; removal of glycine moiety; removal of γ-glutamyl moiety	Glutathione-S-transferase; Phytochelatin synthase; γ-Glutamyl-cyclotransferase	Conjugation kinetics of CMTP and glutathione with F, FMC, and CMTP competing for available GSTs [4,13].
R11: MPMC —>	Removal of MPMC	Unknown	Mass action, this work.
R12: F —> BF	Fenclorim is bound to an insoluble matrix in the medium	Unknown	Mass action, this work.
R13: BF —> FC in cell wall	FC accumulation in the cell wall	Unknown	Mass action, this work.
R14: BF —>	Removal of the bound fenclorim in the medium	Unknown	Mass action, this work.
R15: FC in cell wall <—> FC in the medium	FC transport between medium and cell wall	Unknown	Reversible Michaelis Menten. FC transport process is reversible [4].
R16: FC in the medium —>	Removal of FC from the medium	Unknown	Mass action, this work.
R17: FC in medium <—> FC in cell	FC transport between cell wall and the intracellular solution	Unknown	Reversible Michaelis Menten. FC transport process is reversible [4].

See Fig. 1 caption for the meaning of the abbreviations.
*Lumped reactions.

Experimental data derived from the 0–24 h feeding study with *Arabidopsis* suspension cultures show that when exposed to 100 μM fenclorim, only 7.21 μM of the safener is available in solution in the medium and 3.25 μM in the cells at the time of addition (0 h). The "missing" 89.54 μM fenclorim appears to be non-covalently bound to an insoluble matrix in the cultures. In the model, this "missing" fenclorim is described as bound fenclorim (BF). The BF pool includes all molecules that use fenclorim as precursor, which are not detectable in the medium in our experiments [4]. Therefore, at 0 h, R1, R12 and R14 are the only active reactions since no other fenclorim metabolites are detectable either in the medium or in the cell at 0 h (Fig. 1). After 0 h, all reactions shown in Fig. 1 will be activated. Over time, the only metabolite other than fenclorim observed in the medium was FC, which was observed at 4 h and could be shown to have been exported from the cells, as no FC is formed outside the cell in the medium by biological or chemical means [4]. We have therefore assumed that BF can also not be directly converted into FC in the medium. The mass balance analysis based on the experimental data (Table 1 in [4]) reveals that the FC observed in the medium at 4 h does not directly stem from the intracellular solution. At 0 h, 3.25 μM of total metabolites exist in the cell. However, at 4 h, the total concentrations of all metabolites in the cell have increased to 14.35 μM. As fenclorim concentration in the medium is only reduced by 6.2 μM from 0–4 h and the stoichiometry of all metabolites in the reactions shown in Fig. 1 is unity, there must be an additional source providing FC into the medium. Based on experimental methodology in literature [4], only the extractable FC in the cultures is measured. The current analysis suggests that there must be an additional pool of non-extractable FC which can serve as a subsequent source of soluble FC. Mass balance analysis therefore suggests that FC must be transiently covalently bound to insoluble cell components. Therefore, FC in the medium will be provided through reactions R13, R15 and R17. At 0 h, only fenclorim can be identified as a xenobiotic in the cell, indicating that the safener is not immediately converted into other metabolites. This is consistent with the restricted (uninduced) GST activity determined at 0 h. From 0 to 24 h, the reactions R2 to R11 occur in the cell, leading to the accumulation of the fenclorim metabolites shown in Fig. 1. Therefore, based on the biochemical knowledge and the mass-balance analysis of experimental data, the revised pathway of fenclorim metabolism in *Arabidopsis* suspension cultures is as described (Fig. 1).

2.2. Kinetics

In the model, three reactions (R2, R6 and R10) are mediated by GST-catalysed conjugations. Therefore, the three sets of substrates effectively compete for the available GSTs. Based on the mechanism of GSTs-catalysed bi-substrate reaction [13], the kinetics of the three reactions are derived (v_{R2}, v_{R6} and v_{R10} in Table 2). The competition of the three reactions for GSTs is clearly described by the kinetics. For example, increasing the concentration of either FMC or CMTP decreases v_{R2} because both R6 and R10 also use GSTs as catalyst. *GST*1, *GST*2 and *GST*3 are the maximal enzyme activity for v_{R2}, v_{R6} and v_{R10} and they are related by $GST1 = k_{cat1}[GST]$, $GST2 = k_{cat2}[GST]$ and $GST3 = k_{cat2}[GST]$ where [*GST*] is the total concentration of GSTs. GST activity toward fenclorim was experimentally determined from 0 h to 24 h and increases approximately linearly with time. Due to the lack of information on the safener-induced transcriptional activation of GSTs, it is not possible to model GST activity toward fenclorim based on a

Table 2
Rate equation and parameter values.

Rate equation	Parameter*
$v_{R1} = \frac{\frac{v_{1f}[F\_medium]}{k_{1S}} - \frac{v_{1r}[F\_cell]}{k_{1P}}}{1 + \frac{[F\_medium]}{k_{1S}} + \frac{[F\_cell]}{k_{1P}}}$	$v_{1f}=0.5957\ \mu M\ \min^{-1}$; $v_{1r}=0.3668\ \mu M\ \min^{-1}$; $k_{1S}=86.91\ \mu M$; $k_{1P}=5032.99\ \mu M$;
$v_{R2} = \frac{k_{GST1}[GST]\frac{[F\_cell]}{k_{a1}}\frac{[G]}{k_{a2}}}{1 + \frac{[F\_cell]}{k_{a1}} + \frac{[G]}{k_{a2}} + \frac{[FMC]}{k_{a3}} + \frac{[CMTP]}{k_{a4}} + \frac{[F\_cell]}{k_{a1}}\frac{[G]}{k_{a2}} + \frac{[FMC]}{k_{a3}}\frac{[G]}{k_{a2}} + \frac{[CMTP]}{k_{a4}}\frac{[G]}{k_{a2}}}$	$k_{GST1}=1\ \min^{-1}$; $k_{a1}=3.722\ \mu M$; $k_{a2}=45.03\ \mu M$; $k_{a3}=1.938\ \mu M$; $k_{a4}=9.588\ \mu M$;
$v_{R3} = \frac{v_3\frac{[FG]}{k_{b1}}}{1 + \frac{[FG]}{k_{b1}} + \frac{[FACG]}{k_{b2}}}$	$v_3=0.032\ \mu M\ \min^{-1}$; $k_{b1}=14.41\ \mu M$; $k_{b2}=0.9654\ \mu M$;
$v_{R4} = \frac{v_4\frac{[F\gamma EC]}{k_{4S}}}{1 + \frac{[F\gamma EC]}{k_{4S}}}$	$v_4=0.03349\ \mu M\ \min^{-1}$; $k_{4S}=7.067\ \mu M$;
$v_{R5} = \frac{v_5\frac{[FC]}{k_{5S}}}{1 + \frac{[FC]}{k_{5S}}}$	$v_5=0.03446\ \mu M\ \min^{-1}$; $k_{5S}=3.7167\ \mu M$;
$v_{R6} = \frac{k_{GST2}[GST]\frac{[FMC]}{k_{a3}}\frac{[G]}{k_{a2}}}{1 + \frac{[F\_cell]}{k_{a1}} + \frac{[G]}{k_{a2}} + \frac{[FMC]}{k_{a3}} + \frac{[CMTP]}{k_{a4}} + \frac{[F\_cell]}{k_{a1}}\frac{[G]}{k_{a2}} + \frac{[FMC]}{k_{a3}}\frac{[G]}{k_{a2}} + \frac{[CMTP]}{k_{a4}}\frac{[G]}{k_{a2}}}$	$k_{GST2}=0.00384\ \min^{-1}$; Others are the same as in v_{R2}
$v_{R7} = \frac{v_7\frac{[FACG]}{k_{b2}}}{1 + \frac{[FG]}{k_{b1}} + \frac{[FACG]}{k_{b2}}}$	$v_7=0.0043\ \mu M\ \min^{-1}$; Others are the same as in v_{R3}
$v_{R8}=k_8[FACC]$	$k_8=0.428\text{e-}08\ \min^{-1}$
$v_{R9} = \frac{v_9\frac{[FC]}{k_{9S}}}{1 + \frac{[FC]}{k_{9S}}}$	$v_9=0.002415\ \mu M\ \min^{-1}$; $k_{9S}=0.06632\ \mu M$;
$v_{R10} = \frac{k_{GST3}[GST]\frac{[CMTP]}{k_{a4}}\frac{[G]}{k_{a2}}}{1 + \frac{[F\_cell]}{k_{a1}} + \frac{[G]}{k_{a2}} + \frac{[FMC]}{k_{a3}} + \frac{[CMTP]}{k_{a4}} + \frac{[F\_cell]}{k_{a1}}\frac{[G]}{k_{a2}} + \frac{[FMC]}{k_{a3}}\frac{[G]}{k_{a2}} + \frac{[CMTP]}{k_{a4}}\frac{[G]}{k_{a2}}}$	$k_{GST3}=0.55\ \min^{-1}$; Others are the same as in v_{R2}
$v_{R11}=k_{11}[MPMC]$	$k_{11}=0.0075\ \min^{-1}$
$v_{R12}=k_{12}[F\_medium]$	$k_{12}=0.001638\ \min^{-1}$
$v_{R13}=k_{13}[BF]$	$k_{13}=0.01701\ \min^{-1}$
$v_{R14}=k_{14}[BF]$	$k_{14}=0.00087\ \min^{-1}$
$v_{15} = \frac{\frac{v_{15f}[FC\_CW]}{k_{15S}} - \frac{v_{15r}[FC\_medium]}{k_{15P}}}{1 + \frac{[FC\_CW]}{k_{15S}} + \frac{[FC\_medium]}{k_{15P}}}$	$v_{11f}=2.4058\ \mu M\ \min^{-1}$; $v_{15r}=0.10\ \mu M\ \min^{-1}$; $k_{15S}=176.53\ \mu M$; $k_{15P}=4618.0\ \mu M$;
$v_{R16}=k_{16}[FC\_medium]$	$k_{16}=0.0205\ \min^{-1}$
$v_{17} = \frac{\frac{v_{17f}[FC\_CW]}{k_{17S}} - \frac{v_{17r}[FC\_cell]}{k_{17P}}}{1 + \frac{[FC\_CW]}{k_{17S}} + \frac{[FC\_cell]}{k_{17P}}}$	$v_{17f}=0.03004\ \mu M\ \min^{-1}$; $v_{17r}=0.04519\ \mu M\ \min^{-1}$; $k_{17S}=1.2679\ \mu M$; $k_{17P}=1.1578\ \mu M$;

*No kinetic parameters relating to fenclorim metabolism are available in literature. All parameters are searched using genetic algorithms in the COPASI repository [14].

detailed reaction mechanism. Instead, based on experimental observation [4], we can use the following equation to describe the dependence of GST activity toward fenclorim from 0 to 24 h.

$$GST = GST_a + \frac{2*(GST_b - GST_a)*\text{time}}{k_{GST1} + \text{time}} \quad (1)$$

where $GST_a = 0.0\ \mu M\ \min^{-1}$ is the GST activity at 0 h and $GST_b = 36.0\ \mu M\ \min^{-1}$ is the activity at 24 h, with these values estimated on experimental data [4]. The constant $k_{GST1} = 1440$ min, refers to the time when the last measurement was conducted. Eq. (1) approximately describes the experimental relation between GST activity toward fenclorim and time. Accordingly, GST activity toward both FAC and CMTP also increases with time. Effects of both GST_a and GST_b on the transient dynamics of fenclorim metabolism will be investigated in the Result section. In addition, the respective disassociation constant is the same in v_{R2}, v_{R6} and v_{R10}.

The four steps described as R6–R10 are lumped reactions. For example, R6 is the net reaction of the following two reactions: R6a: FMC —> FAC + carboxyl; and R6b: FAC+ G —> FACG. These reactions have to be combined as FAC is not experimentally detectable. Lumping the two reactions into R6 in Table 1 implies that FAC is assumed to be at steady state. Once FAC is experimentally measured, R6 could be resolved into two reactions (R6a and R6b) and the model modified accordingly.

Three reactions (R3, R7 and R10) potentially compete for the conjugate processing enzyme phytochelatin synthase. However, in R10 the reaction using phytochelatin synthase to remove the glycine moiety is assumed to be at steady state and as such this reaction R10 does not need to be considered. In contrast, the kinetics of R3 and R7 are based on their competition for phytochelatin synthase and are related to the total concentration of the enzyme. Similarly, reactions R4, R7 and R10

compete for γ-glutamylcyclotransferase. Since R7 and R10 are lumped reactions, their competition for γ-glutamylcyclotransferase is not considered with R4's kinetics described using irreversible Michaelis–Menten kinetics.

Reactions R1, R15 and R17 describe transport processes across the cell membrane and reversible Michaelis–Menten kinetics are employed to model the three processes. All other reactions are assumed to follow either irreversible Michaelis–Menten or mass-action kinetics.

2.3. Parameter estimation

Parameters are searched using genetic algorithms in the COPASI repository [14]. A typical searching setting is as follows. Number of generation: 20,000; population size: 1000, random number generator: 1. Experimental data for 24 h [4] are used to calculate mean square. Other settings are tested by using a different number of generation and population size, with a similar mean square obtained. Parameters are also searched using evolutionary programming, but no better parameter sets are found. Fig. 2 shows the comparison between model calculations and two sets of experimental results. The first set of experimental data is 0–24 h measurements (4 data points for each metabolite, at 0 h, 4 h, 8 h, and 24 h respectively) [4], which are used for parameter searching. The second set of experimental data is derived from previously unpublished 0–4 h measurements (5 data points, at 0 h, 0.5 h, 1 h, 2 h and 4 h respectively) obtained using the sampling and assay methods described [4]. Experimentally, the reproducibility for 0–4 h measurements is poor, and the associated data noisy. Therefore, the data for 0–4 h measurements are not used when parameter searching is conducted, but are included for the purpose of comparison. Based on the parameter values obtained, the modelling results are compared with experimental data as follows. For all metabolites in the cell, modelling results are in good agreement with the experimental measurements (Fig. 2a–c). However, the discrepancy between experimental results and modelling results for FC in the medium is relatively large (Fig. 2d). In order to examine if this discrepancy is caused by using reversible Michaelis–Menten kinetics to describe transport across the membrane, different known types of kinetics (mass-action, reversible Michaelis–Menten, irreversible Michaelis–Menten, irreversible Michaelis–Menten with substrate inhibition, reversible Michaelis–Menten with substrate inhibition) which are generally used to describe chemical transport across the cell membrane, are tested to describe the transport of FC between the cell wall and the intracellular solution and/or the transport of FC between the cell wall and the medium (reactions R15 and R17). For the parameter values searched by using genetic algorithms, the five types of kinetics lead to the similar trend for FC concentration in the medium, confirming that the discrepancy between experimental results and modelling results is not caused by the kinetics type. Therefore, the modelling results imply that the experimental measurements of FC have not taken all FC in the medium into account. Based on experimental methodology in literature [4], only the FC in the solution is measured. However, as discussed above, it is possible that FC could be covalently bound to cell components, with this part of the FC being undetectable. Therefore, it is concluded that the difference between the calculated and measured FC in the medium (Fig. 2d) is the FC "bound" within the matrix. Therefore, experimental measurement has not measured all FC in the medium. Since the transient dynamics of all metabolites in the cell are well fitted into the model by using the 0–24 h experimental data (in particular, it should be noted that experimental data are with a typical error ~20–30%.), it is reasonable to consider that in the developed model (Fig. 1), the kinetics and the searched parameters (Table 2) have captured the main features of the experimental system.

3. Results

3.1. Transient dynamics of fenclorim metabolism and effects of GST expression

Fenclorim metabolism can be analysed using the kinetic model. Fig. 3 shows how the initial concentration of the safener in the

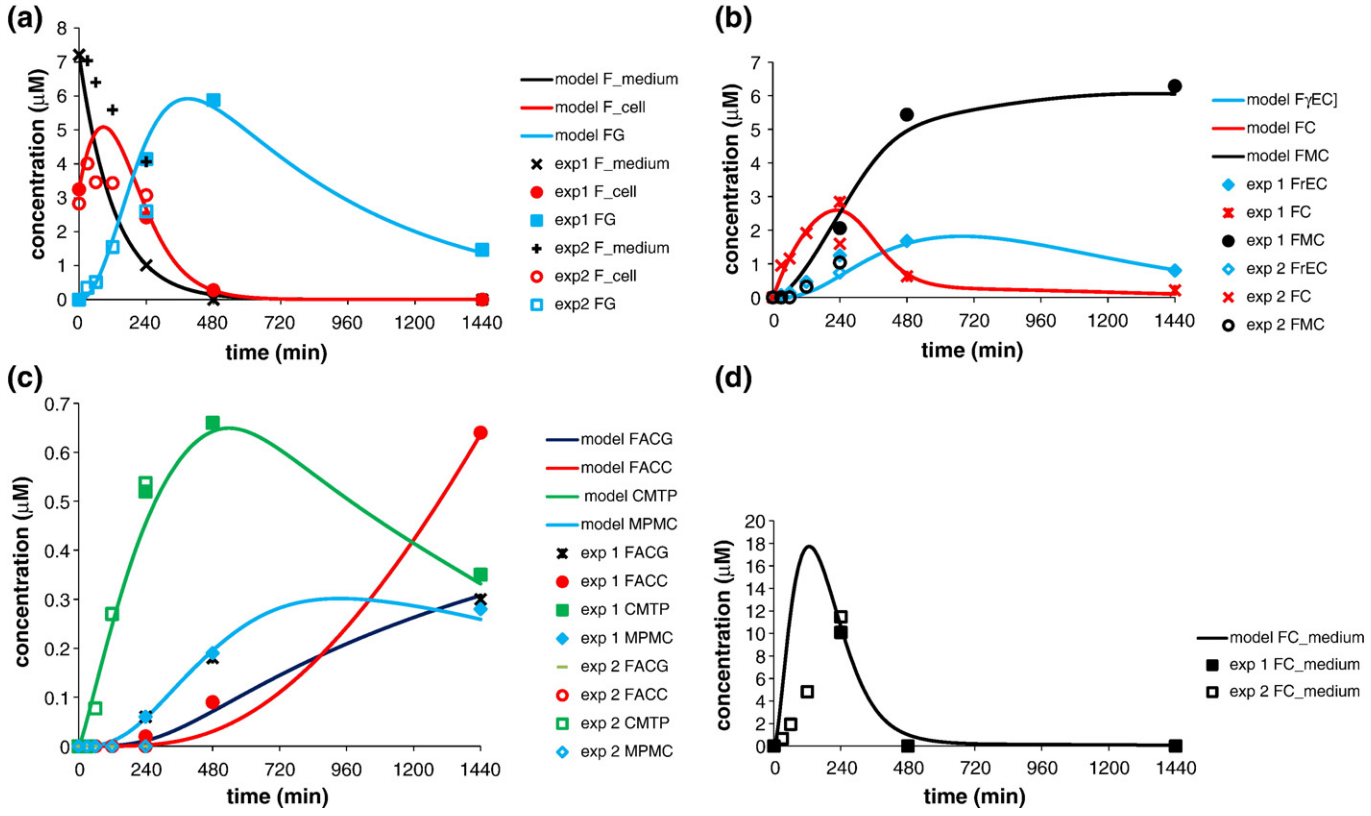

Fig. 2. Comparison of experimental data for two experimental setups (experiment 1, in [4]; experiment 2: this work) with computational results using the kinetic model (Fig. 1, Tables 1 and 2).

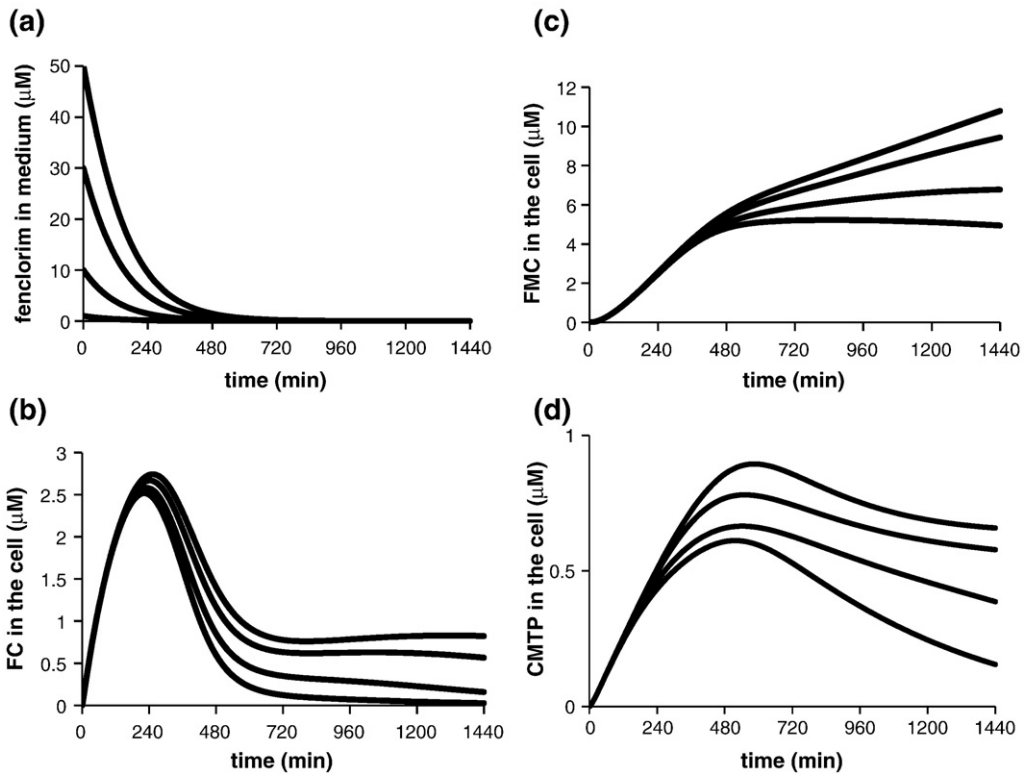

Fig. 3. Effects of fenclorim concentration in the medium on the transient dynamics of fenclorim metabolism. a): fenclorim in the medium; (b): FC in the cell; c): FMC in the cell, d) CMTP in the cell. In (a)–(d) and curves from bottom to top, initial fenclorim concentration in the medium is 1 μM; 10 μM; 30 μM; 50 μM, respectively.

medium affects the transient dynamics of fenclorim metabolism. For different external fenclorim concentrations, fenclorim concentration always monotonically decreases with time. However, before 4 h, increasing the concentration of fenclorim in the medium approximately does not affect FC concentration and therefore, the levels of the downstream metabolites such as FMC, CMTP. However, after 4 h, FC concentration is markedly altered by different fenclorim concentrations in the medium. The results show that it takes approximately 4 h for the fenclorim in the medium to propagate to its downstream metabolites (e.g. FC, FMC, CMTP).

Effects of glutathione concentration in the cell on the transient dynamics can also be analysed. Fig. 4 shows that although glutathione concentration in the cell significantly affects the dynamics of fenclorim, FMC and CMTP in the cell, it has only limited effects on FC dynamics. This reflects i) glutathione directly conjugates with fenclorim, FMC and MPMC in the cell, and ii) effects of glutathione on FC is secondary via its effect on fenclorim dynamics in the cell. Using the metabolic model, the quantitative trend of all metabolites relating to fenclorim metabolism can be predicted, as shown in Figs. 3 and 4.

From 0 to 24 h, GST activity toward fenclorim monotonically increases from $GST1_a$ to $GST1_b$ following Eq. (1). However, Fig. 5a shows that the reaction rate v_{R2}, v_{R6} and v_{R10} change differently with time, reflecting the concentrations of both GST enzymes and metabolites control reaction fluxes. As GST activity toward fenclorim increases, v_{R2} initially also increases, reflecting that GST activity positively regulates the flux. Then v_{R2} decreases, reflecting that GST activity negatively regulates the flux by reducing fenclorim concentration and increasing FMC and CMTP concentration simultaneously. Similarly, there is an initial increase phase and a decrease phase in v_{R10}. However, from 0–24 h, v_{R6} monotonically increases, reflecting that GST activity always positively regulates flux. It is clear that, although GST activity toward fenclorim monotonically increases, the compounded effects of both GST activity and metabolite concentrations on metabolic fluxes lead to the different time-course trends for different all metabolites.

Fig. 5b and c summarize how GSTs expression patterns affect transient dynamics. By increasing GST_b, GST activity increases more quickly. In general, over a shorter time, increasing GST_b does not affect the transient dynamics, although GST_b may have different effects on levels of different metabolites over this period. Fig. 5b and c show that fenclorim in the cell and FMC transient dynamics does not markedly change at a timescale of 2 h and 6 h respectively, when GST_b changes from 10 μM $\min^{-1}$ to 70 μM $\min^{-1}$ (a 7-fold increase). GST_a represents the background expression of GSTs prior to induction by fenclorim. As shown in Fig. 4, as GST_a increases from 0 to 3 μM $\min^{-1}$, although GST_a markedly affects fenclorim transient dynamics, it only slightly affects the transient dynamics of FMC and CMTP (data not shown).

It is clear that the model is able to quantitatively analyze the transient dynamics of fenclorim metabolism. Different time-course trends for all metabolites can be understood in terms of the compounded effects of both GST activity and metabolite concentrations on metabolic fluxes. Moreover, the model can analyze the time scale for the conversion of fenclorim into its downstream metabolites. In addition, the effects of GST expression patterns on the transient dynamics can be analyzed using the model. However, the current model is based on transient experimental data, with the only steady state for the model being one in which all metabolite concentrations are zero. Such a steady state is trivial both experimentally and theoretically. Therefore, in order to study the steady state and sustained dynamics of fenclorim metabolism, the model is further developed to allow non-zero stable states to be established. Subsequently, the steady state and sustained dynamics of the fenclorim metabolism system can be analyzed.

3.2. Steady state

In order for fenclorim metabolism to establish a non-zero stable state, fenclorim concentration in the medium must remain at a constant concentration. This can be experimentally realized in a

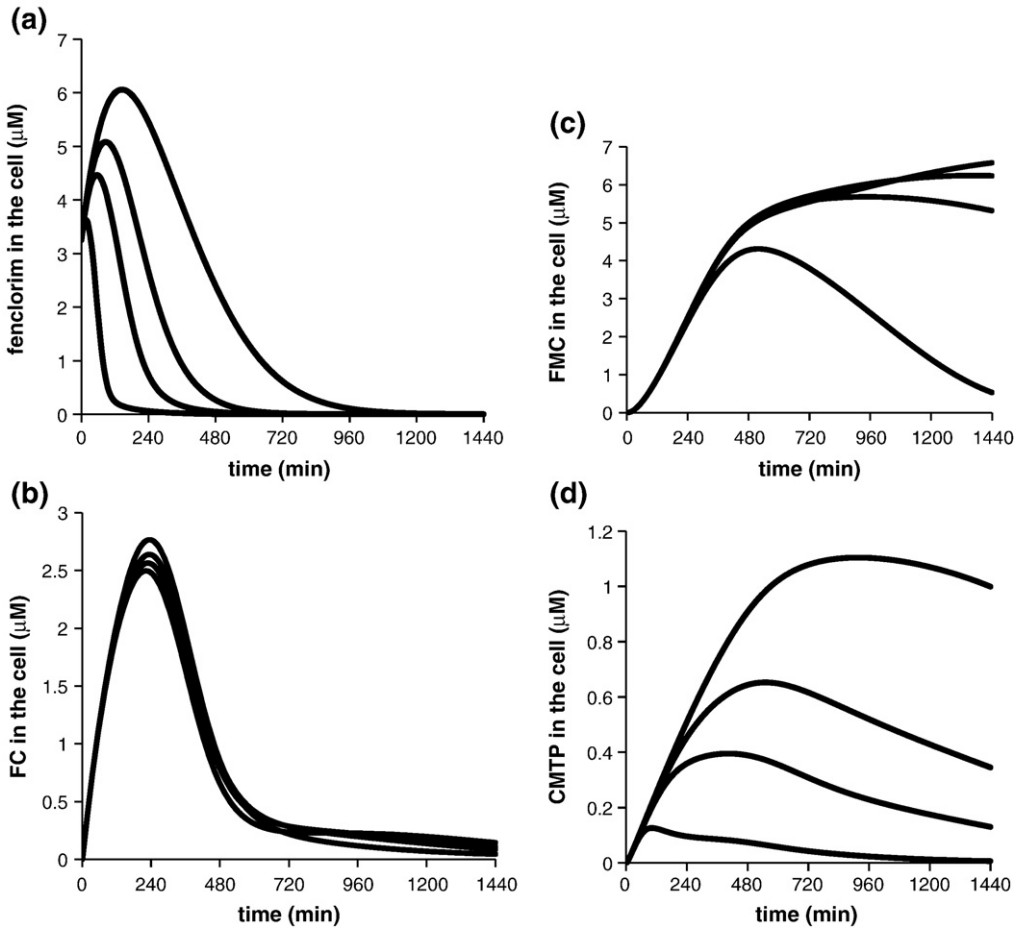

Fig. 4. Effects of glutathione concentration in the cell on the transient dynamics of fenclorim metabolism. a): fenclorim in the medium; (b) FC in the cell; c) FMC in the cell; d) CMTP in the cell. In (a)–(d) and curves from top to bottom, glutathione concentration in the cell is 0.2 μM; 0.5 μM; 1 μM; 5 μM, respectively.

number of ways. First, the fenclorim medium can be buffered by an external pool. Second, fenclorim is continuously supplied into the medium by feeding it into the medium. Theoretically, these experimental designs are equivalent. In the following, we assume that the fenclorim is supplied to the medium with a constant rate, v_{input}.

$$v_{\text{input}} = k^*[F\_\text{external}] \tag{2}$$

where k is the rate constant and [*F_external*] is the fenclorim concentration in the external pool.

Once fenclorim concentration in the medium establishes a steady state, GST activity also establishes a steady state which is related to the concentration of the safener in the medium. Experimentally, it has been shown that GST activity approximately establishes a steady state after a 24 h exposure to safener. We can then use the experimental data of GST activity toward fenclorim at 24 h [4], to establish an approximate relation between the external fenclorim concentration and GST activity toward fenclorim.

$$GSTss = \frac{GST_f{}^*[F\_\text{external}]}{k_f + [F\_\text{external}]} \tag{3}$$

Based on the Fig. 1C in [4], $GST_f = 72\ \mu M\ \text{min}^{-1}$; $k_f = 100\ \mu M$. Eq. (3) shows that, for [*F_external*] = 100 μM, $GSTss = 36\ \mu M\ \text{min}^{-1}$, which describes the experimental induction pattern of GST activity determined toward fenclorim at 24 h *in planta* [4].

After incorporating Eqs. (2) and (3) into the model, fenclorim metabolism is able to establish non-zero steady states. Subsequently, we can use the model to study the steady-state properties and dynamics of fenclorim metabolism.

3.3. Flux regulation at steady states

The flux through fenclorim metabolism is controlled by gene expression (GST activity) and metabolic regulation (the interaction between GST-catalysed reactions with the rest of fenclorim metabolism and the competition of GSTs availability between different substrates, notably fenclorim, FAC and CMTP). An important question is how GST expression regulates the flux, when the external fenclorim concentration changes. Therefore, we analyse to what extent the fluxes in fenclorim metabolism are regulated by GST expression or by metabolic regulation following the method developed by Rossell et al. [15,16].

By increasing external fenclorim concentration by a certain amount (here 5 μM) each time, the dependence of "hierarchical regulation coefficient that quantifies how GST activity affects fenclorim metabolic fluxes in response to altering the supply of safener is determined. Fig. 6 reveals that as external fenclorim concentration increases up to 60 μM, the flux of CMTP to MPMC is purely regulated by GST activity ($0.9 < \rho_{h(R10)} < 1.1$), while the flux of fenclorim in the cell to FG and the flux of FMC to FACG are cooperatively regulated by GST activity and by metabolic regulation ($0 << \rho_{h(R2)} << 1$ and $0 << \rho_{h(R6)} << 1$). Therefore, both GST activity and the interaction of the associated catalysed reactions with the rest of the fenclorim metabolism positively regulate the two fluxes. As external fenclorim concentration increases from 60 μM to 95 μM, the

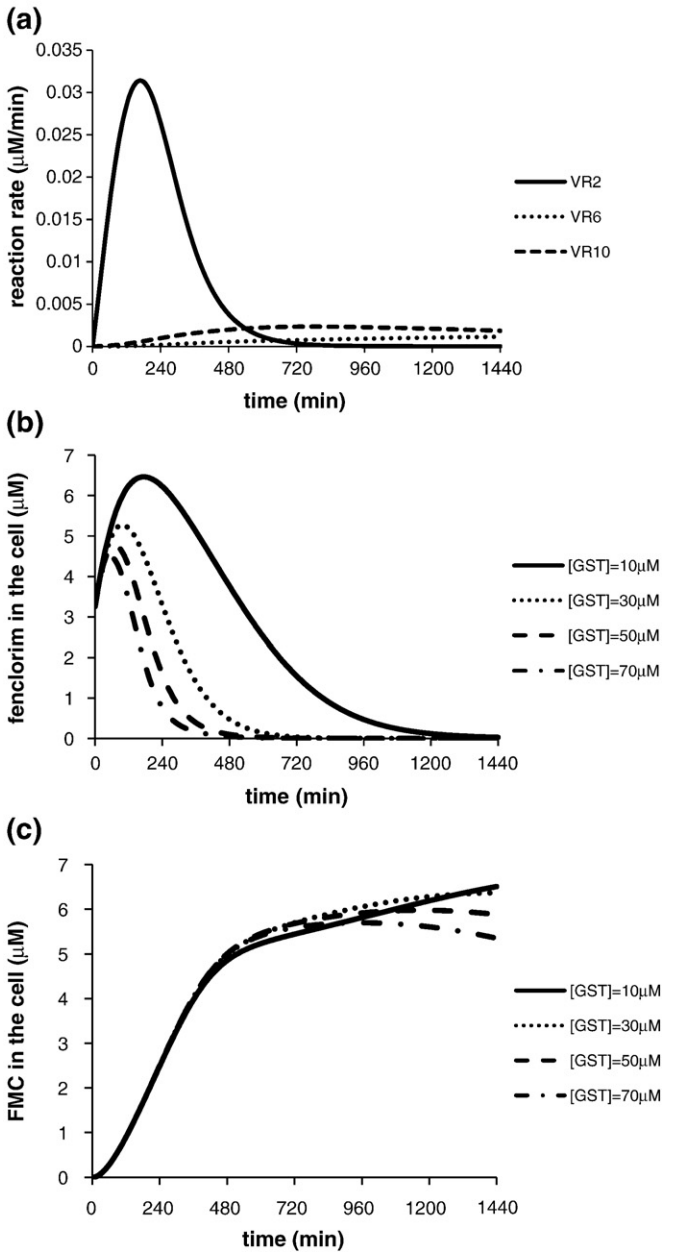

Fig. 5. Transient fluxes for three GST conjugation reactions (R2, R6, and R10 in Fig. 1) (a) and effects of GST expression patterns on the transient dynamics of fenclorim metabolism (b, c).

flux regulation has shifted. Although GST activity and metabolic regulation still play a cooperative role in the flux of fenclorim conjugation to form FG and the flux of FMC to FACG, the flux of CMTP to MPMC becomes positively regulated by GST activity and negatively regulated by metabolic interaction ($\rho_{h(R10)} >> 1$). As external fenclorim concentration further increases, the flux of FMC to FACG becomes purely GST-activity regulated and the negative metabolic regulation diminishes ($0.9 < \rho_{h(R6)} < 1.1$). However, GST activity and metabolic regulation play antagonistic roles both in the flux of CMTP to MPMC and in the flux of fenclorim in the cell being metabolized to FG: both fluxes are mainly directed by GST activity, but counteracted by metabolic interaction ($\rho_{h(R2)} >> 1$ and $\rho_{h(R10)} >> 1$). It is clear that, although GST activity is monotonically enhanced as external fenclorim concentration increases, the role of GST activity in regulating fluxes may be different. The kinetic model is able to quantitatively understand and analyse how fenclorim metabolic fluxes are regulated when the external concentration of the safener changes.

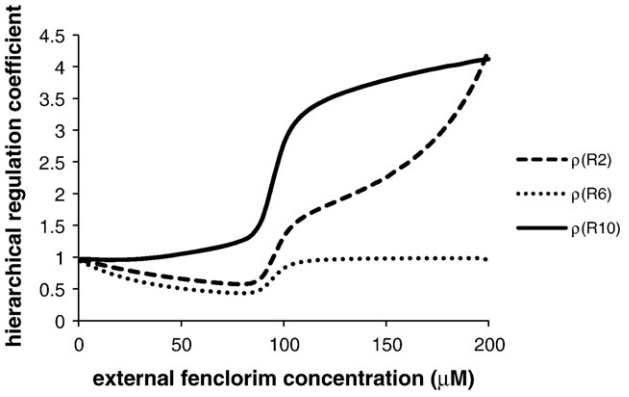

Fig. 6. Hierarchical regulation coefficients for three GST conjugation reactions (R2, R6, and R10 in Fig. 1). Starting from 1 μM, external fenclorim concentration increases 5 μM each time, two steady states for two neighboring external fenclorim concentrations are compared. The rate constant for supplying fenclorim to medium is $k = 5.7\ e-5\ \mathrm{min}^{-1}$.

3.4. Steady-state response to external fenclorim concentration

The kinetic model provides opportunities to examine how steady-state concentrations of metabolites in the cell are related to the external fenclorim concentration. Fig. 7 shows that different metabolites in the cell have different responses to the availability of fenclorim. As external fenclorim increases up to 100 μM, the steady state concentration of fenclorim and CMTP remain low. However, further increases in external fenclorim concentration leads to a drastic increase in the steady state concentration of both fenclorim and CMTP. In addition, both FC and FG concentration remain low as external fenclorim increases up to 200 μM. These results imply that the levels of fenclorim fed to the cells will only define the high concentrations of certain metabolites in the cell. It is possible to control the relative levels of certain metabolites by adjusting external fenclorim concentration.

3.5. Dynamics

In fenclorim metabolism, there are a number of reactions competing for the same enzymes, posing the question if such processing is capable of generating dynamical patterns? Stability analysis reveals that for the parameter values shown in Table 2, the steady state is stable and no dynamical patterns emerge. However, by changing parameter values, oscillatory dynamics can emerge. Fig. 8a shows the bifurcation diagram

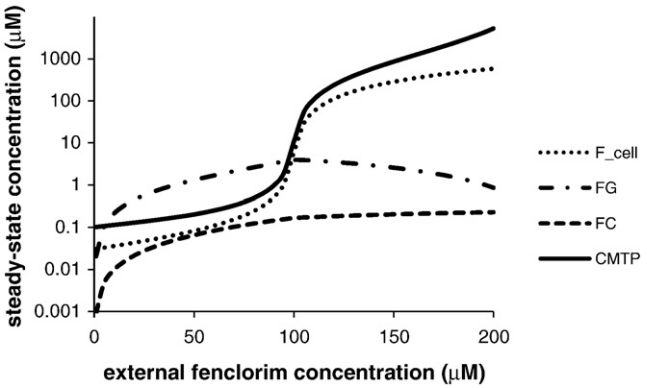

Fig. 7. Effects of external fenclorim concentration on steady-state values of four metabolites. The rate constant for supplying fenclorim to medium is $k = 5.7\ e-5\ \mathrm{min}^{-1}$.

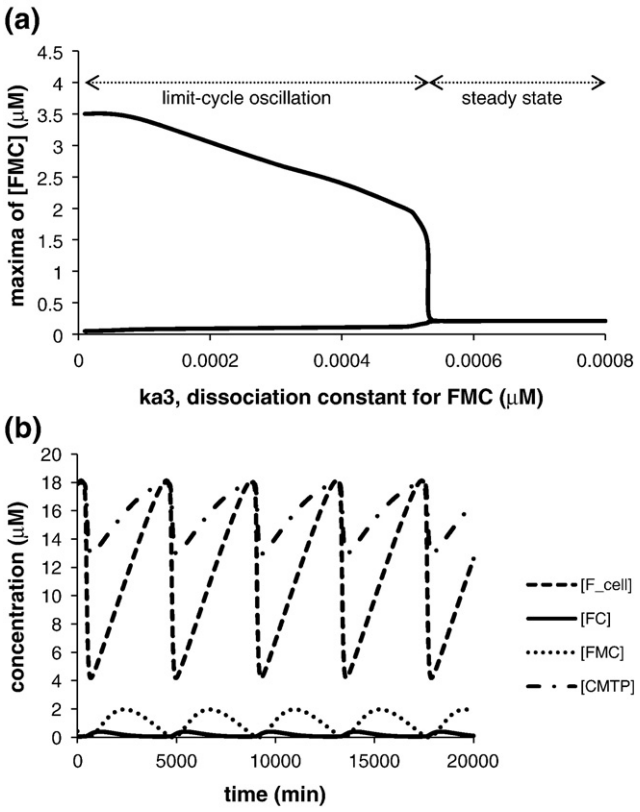

Fig. 8. Generation of limit-cycle oscillation by changing parameter k_{a3}, the dissociation constant for FMC. a) bifurcation diagram. other parameters are the same as in Table 2. b) an example of oscillatory dynamics for fenclorim metabolism. $k_{a3} = 0.0005\ \mu M$. The rate constant for supplying fenclorim to medium is $k = 5.7\ e-5\ \mathrm{min}^{-1}$.

by changing the value of one parameter (k_{a3}, dissociation constant of FMC to GST). It reveals that when $k_{a3} \geq 0.000531\ \mu M$, the system maintains a stable steady state. However, when $k_{a3} < 0.000531\ \mu M$, fenclorim metabolism generates oscillatory patterns. By comprehensively searching for other chosen parameters, complex oscillations and chaos are not observed. Therefore, the system of fenclorim metabolism may only support simple oscillatory dynamics. Fig. 8b shows an example of oscillatory dynamics for $k_{a3} = 0.0005\ \mu M$ (all other parameter values as in Table 2). As the values of all kinetic parameters depend on environmental factors such as temperature, the parameter values under different environmental conditions may be significantly different from the values shown in Table 2. Therefore, oscillatory dynamical patterns for fenclorim metabolism may also become possible if environmental conditions change.

4. Conclusion and discussion

A kinetic model for the metabolism of herbicide safener fenclorim has been developed in *Arabidopsis* cultures based on experimental measurements. It is demonstrated that, based on the kinetics of each process, the model has captured the main features of fenclorim metabolism *in planta*. The kinetic model is able to analyse the dynamics of fenclorim metabolism and how each related metabolite in the cell depends on external fenclorim concentration, GST activity and glutathione concentration. A unique aspect of the work is the modelling of how safener metabolism responds to changes in GST expression, addressing the question to what extent is fenclorim autoregulating its own metabolism. Following fenclorim application, fenclorim metabolism and GST expression evolve simultaneously with time. Analysis of the model showed that the regulation of flux though the glutathione conjugation pathway by GSTs shifted as the external concentrations of fenclorim were altered. In addition, analysis of the model also shows that fenclorim metabolism may generate complicated dynamics such as oscillations if kinetic parameter values are allowed to vary. Generally speaking, environmental factors such as temperature are important factors affecting the values of kinetic parameters. When fenclorim metabolism takes place under different environmental conditions, one would expect that different parameter values would be realised due to changes in the temperature. As the underlying mechanism of fenclorim metabolism supports the generation of oscillatory dynamics, how the dynamics of fenclorim metabolism responds to a changing environment is an intriguing question which remains to be addressed. Whether or not oscillatory dynamics can emerge from fenclorim metabolism depends on how environmental conditions affect the values of parameters.

Although the fenclorim metabolism process is experimentally determined [4], its kinetic parameters have not been experimentally known. In the model developed, there are 35 parameters and 11 measured metabolites at four time points in both the culture medium and in the cell (in total, 44 experimental data points were measured). The kinetic model is an underdetermined dynamical system. Genetic algorithms is a global optimisation methodology [17,18]. It is generally used for parameter searching for biological systems and it can be effectively applied to underdetermined systems [17,18]. In this work, genetic algorithms in the COPASI repository [14] is used to search for all parameters based on experimental measurements [4] due to the lack of experimental values of kinetic parameters. As the kinetic system is underdetermined, it is possible to generate multiple parameter sets when parameter searching using genetic algorithms is implemented. In particular, initial conditions of metabolites in the model and the settings in genetic algorithms [14] are two important factors that affect the outcome of parameter searching. We have dealt with the two factors as follow. First, the experimentally measurable concentrations of all 11 metabolites at zero time point are used as initial conditions of metabolites in the model. By doing so, initial conditions of metabolites in the model are set to be the experimental values, and therefore their effects were not further investigated. Second, number of generation and population size in the settings of genetic algorithm may affect the outcome of parameter searching. We compared different settings initially and then chose a specific setting (number of generation: 20,000; population size: 1000, random number generator: 1). The searched parameters are included in Table 2. As the model with the searched parameters can quantitatively reproduce the experimental trend of all metabolites in the cell, we consider that the model has captured the main features of fenclorim metabolism.

The number of the freedoms in the kinetic model could be reduced by either theoretically reducing the number of parameters or experimentally increasing the number of measured metabolites. During the model development, we use Michaelis–Menten type of enzyme kinetics for the processes with known enzymes to avoid the loss of biological significance. For the processes with unknown enzymes, we use simple mass-action kinetics to reduce the number of parameters. Therefore, the resulted model is the result after balancing biological significance and the number of parameters. In general, describing biological reality in detail favours a model with more parameters and parameterising the model based on experimental measurements favours a model with fewer parameters. A careful balance needs to be reached when a kinetic model is developed. Experimentally, it is also possible to reduce the number of freedoms by increasing the number of measurable metabolite forms. For example, molecules labelled with stable isotopes can be used to increase the number of the measurable forms of a metabolite and therefore to reduce the number of freedoms [19,20]. However, to our knowledge, molecules labelled with stable isotopes have not been used to study the metabolism of herbicide and safener. This indicates that the quantitative resolution of herbicide and safener metabolism

may require novel experimental designs with the consideration of quantitative modelling development in the future.

The predictive modelling of the metabolism and disposition of xenobiotics in animals is a well established component of the process of drug development (reviewed by Lave et al. [21]). In mammalian systems predictive modelling has been used to address a number of key questions at the various stages of the drug-discovery and -development process and can be used to assess the risk of metabolites accumulating which can cause diseases such as cancer [22]. A key component of such modelling is factoring in the potential for drugs to induce detoxifying enzymes and the effect this enhancement in metabolism has on clinical efficacy [21]. In plants, the inducible metabolism of crop protection agents by agents such as safeners has been recorded in the literature for over 20 years (reviewed by Edwards et al. [11]), though to our knowledge, the consequences of such enhancement have not been the subject of metabolic modelling. A predictive understanding of how safeners can alter flux through detoxification pathways and regulate the accumulation of related metabolites would be a useful tool in understanding how to use these compounds most effectively to enhance herbicide metabolism in cereals and hence alter selectivity. Of direct relevance to this report, the majority of chloroacetanilide and thiocarbamate herbicides which are safened in cereals undergo GST-mediated detoxification, with the rates of metabolism enhanced by safener-treatment [2]. Intriguingly in the case of safeners such as fenclorim and benoxacor which are themselves metabolized by GSTs [4,7] these compounds would effectively compete for the detoxifying enzymes with the co-applied herbicides adding a further dimension to the required modelling. It will now be of interest to develop predictive tools to describe the combined inducible metabolism of both safeners and herbicides by GSTs in *Arabidopsis* cultures and cereal crops.

Using deterministic rate laws and differential equations, this paper has developed a quantitative model for fenclorim metabolism. When a cellular system is modelled, an alternative methodology is stochastic modelling [23,24]. A future development for modelling inducible metabolism of both safeners and herbicides by GSTs may include the effects of stochasticity, in particular, when concentrations are very low.

References

[1] J. Davies, J.C. Caseley, Herbicide safeners: a review, Pestic. Sci. 55 (1999) 1043–1058.
[2] K.K. Hatzios, N. Burgos, Metabolism-based herbicide resistance: regulation by safeners, Weed Sci. 52 (2004) 454–467.
[3] R. Edwards, D. Del Buono, M. Fordham, M. Skipsey, M. Brazier, D.P. Dixon, I. Cummings, Differential induction of glutathione transferases and glucosyltransferases in wheat, maize and *Arabidopsis thaliana* by herbicide safeners, Zeitschrift Naturforschung 60 (2005) 307–316.
[4] M. Brazier-Hicks, K.M. Evans, O.D. Cunningham, D.R.W. Hodgson, P.G. Steel, R. Edwards, Catabolism of glutathione conjugates in *Arabidopsis thaliana*: role in metabolic reactivation of the herbicide safener fenclorim, J. Biol. Chem. 283 (2008) 21102–21112.
[5] F. Deng, K.K. Hatzios, Characterization and safener induction of multiple glutathione *S*-transferases in three genetic lines of rice, Pestic. Biochem. Physiol. 72 (2002) 24–39.
[6] S.R. Baerson, A. Sánchez-Moreiras, N. Pedrol-Bonjoc, M. Schulz, I.A. Kagan, A.K. Agarwal, M.J. Reigosa, S.O. Duke, Detoxification and transcriptome response in Arabidopsis seedlings exposed to the allelochemical benzoxazolin-2(3*H*)-one, J. Biol. Chem. 280 (2005) 21867–21881.
[7] B.P. DeRidder, D.P. Dixon, D.J. Beussman, R. Edwards, P.B. Goldsbrough, Induction of glutathione *S*-transferases in *Arabidopsis* by herbicide safeners, Plant Physiol. 130 (2002) 1497–1505.
[8] R. Blum, A. Beck, A. Korte, A. Stengel, T. Letzel, K. Lendzian, E. Grill, Function of phytochelatin synthase in catabolism of glutathione-conjugates, Plant J. 49 (2007) 740–749.
[9] N. Ohkama-Ohtsu, P. Zhao, C. Xiang, D.J. Oliver, Glutathione conjugates in the vacuole are degraded by γ-glutamyl transpeptidase GGT3 in Arabidopsis, Plant J. 49 (2007) 878–888.
[10] N. Ohkama-Ohtsu, A. Oikawa, P. Zhao, C. Xiang, K. Saito, D.J. Oliver, A Gamma-glutamyl transpeptidase-independent pathway of glutathione catabolism to glutamate via 5-oxoproline in Arabidopsis, Plant Physiol. 148 (2008) 1603–1613.
[11] R. Edwards, M. Brazier, D.P. Dixon, I. Cummins, Chemical manipulation of antioxidant defences in plants, Adv. Bot. Res. 42 (2005) 1–32.
[12] A.E. Wolf, K.J. Dietz, P. Schröder, Degradation of glutathione S-conjugates by a carboxypeptidase in the plant vacuole, FEBS lett. 384 (1996) 31–34.
[13] V. Leskovac, Comprehensive enzyme kinetics, Kluwer Academic/Plenum Publishers, 2003.
[14] S. Hoops, S. Sahle, R. Gauges, C. Lee, J. Pahle, N. Simus, M. Singhal, L. Xu, P. Mendes, U. Kummer, COPASI—a COmplex PAthway Simulator, Bioinformatics 22 (2006) 3067–3074.
[15] S. Rossell, C.C. van der Weijden, A.L. Kruckeberg, B.M. Bakker, H.V. Westerhoff, Hierarchical and metabolic regulation of glucose influx in starved *Saccharomyces cerevisiae*, FEMS Yeast Res. 5 (2005) 611–619.
[16] S. Rossell, C.C. van der Weijden, A. Lindenbergh, A. van Tuijl, C. Francke, B.M. Bakker, H.V. Westerhoff, Unraveling the complexity of flux regulation: a new method demonstrated for nutrient starvation in *Saccharomyces cerevisiae*, Proc. Natl. Acad. Sci. U. S. A. 103 (2006) 2166–2171.
[17] D. Goldberg, Genetic algorithms in search, optimisation and machine learning, Addison-Wesley, Reading, MA, 1989.
[18] M. Mitchell, An introduction to genetic algorithms, MIT press, 1996.
[19] A. Roschera, N.J. Krugera, R.G. Ratcliffe, Strategies for metabolic flux analysis in plants using isotope labelling, J. Biotechnol. 77 (2000) 81–102.
[20] C.J. Baxtera, J.L. Liu, A.R. Fernie, L.J. Sweetlove, Determination of metabolic fluxes in a non-steady-state system, Phytochemistry 68 (2007) 2313–2319.
[21] T. Lave, N. Parrott, H.P. Grimm, A. Fleury, M. Reddy, Challenges and opportunities with modelling and simulation in drug discovery and drug development, Xenobiotica 37 (2007) 1295–1310.
[22] P.S. Crooke, M.D. Ritchie, D.L. Hachey, S. Dawling, N. Roodi, F.F. Parl, Estrogens, enzyme variants, and breast cancer: a risk model, Cancer Epidemiol. Biomark. Prev. 15 (2006) 1620–1629.
[23] T.E. Turner, S. Schnell, K. Burrage, Stochastic approaches for modelling in vivo reactions, Comput. Biol. Chem. 28 (2004) 165–178.
[24] M. Perc, A.K. Green, C.J. Dixon, M. Marhl, Establishing the stochastic nature of intracellular calcium oscillations from experimental data, Biophys. Chem. 132 (2008) 33–38.